

Many-body treatment of the collisional frequency shift in fermionic atoms

A.M. Rey¹, A.V. Gorshkov², C. Rubbo¹

¹*JILA, NIST and Department of Physics, University of Colorado Boulder, CO 80309, and*

²*Physics Department, Harvard University, Cambridge, MA, 02138*

(Dated: November 10, 2018)

Recent clock experiments have measured density-dependent frequency shifts in polarized fermionic alkaline-earth atoms using 1S_0 - 3P_0 Rabi spectroscopy. Here we provide a first-principles non-equilibrium theoretical description of the interaction frequency shifts starting from the microscopic many-body Hamiltonian. Our formalism describes the dependence of the frequency shift on excitation inhomogeneity, interactions, and many-body dynamics, provides a fundamental understanding of the effects of the measurement process, and explains the observed density shift data. We also propose a method to measure the second of the two 1S_0 - 3P_0 scattering lengths, whose knowledge is essential for quantum information processing and quantum simulation applications.

PACS numbers: 03.75.Ss, 06.30.Ft, 06.20.fb, 32.30-r, 34.20.Cf

Experimental efforts in cooling, trapping, and manipulating alkaline-earth-like atoms such as Sr and Yb have led to unprecedented developments in optical clocks based on the 1S_0 - 3P_0 transition [1, 2, 3, 4, 5, 6, 7, 8, 9, 10]. While the interrogation of a large number of atoms enhances the sensitivity of these clocks, the accompanying interatomic interactions degrade clock precision. Thus the understanding of these interactions is crucial for precision spectroscopy. Fermionic alkaline-earth atoms have also started to attract considerable theoretical attention in the context of quantum information processing [11, 12, 13, 14] and quantum simulation [15], applications requiring the knowledge of both 1S_0 - 3P_0 scattering lengths. Here we present a many-body formulation, which, on the one hand, allows us to understand the nature of the collisional frequency shift (CFS) measured in a recent experiment [3], and on the other, allows us to propose a way to measure the remaining 1S_0 - 3P_0 scattering length, which was not probed in Ref. [3]. Our model helps to clarify the role of excitation inhomogeneities, dynamics, and interactions in fermionic clock experiments [3, 16, 17, 18].

Clock experiments based on Rabi interrogation start with a nuclear-spin-polarized sample of atoms prepared (for consistency with Ref. [3], which we aim to model) in an excited state e , which is then transferred to the ground state g by illuminating the atoms during a time t_f with a probe beam detuned from the atomic resonance. The CFS $\delta\omega_{eg}$ is inferred by recording the final population in g as a function of the detuning and looking for changes in the corresponding lineshape due to interactions. So far most treatments of CFSs in dilute polarized fermionic gases away from the unitarity limit were based on a static mean field analysis [16, 17, 19, 20]. The latter predicts a frequency shift $\delta\omega_{eg} = \frac{4\pi\hbar a_{eg}^-}{M}(\rho_g - \rho_e)G_{ge}^{(2)}$, with $G_{ge}^{(2)}$ the two atom correlation function at zero distance, which measures the probability that two particles are simultaneously detected, a_{eg}^- the s -wave scattering length between the g and e atoms with mass M , and $\rho_{g,e}$ the corresponding atom densities. Here we extend this formulation beyond mean-field and fully account for the many-body dynamics during Rabi interrogation. Our key statements are as follows. (i) Motion-induced excitation inhomogeneity can lead to s -wave

CFS even in an initially polarized ensemble of fermions. (ii) CFS is sensitive to the time-averaged population difference between g and e atoms, consistently with the mean field approximation, and in particular vanishes when this difference goes to zero (π pulse). (iii) For a fixed pulse area, the CFS approaches zero as $t_f \rightarrow 0$, meaning that, in order to experience interactions, atoms should have enough time to feel the excitation inhomogeneity. (iv) Measurements of $\delta\omega_{eg}$ done by locking the interrogation laser at fixed final ground state fraction are very sensitive to the pulse area and strength of interactions. Depending on these parameters, even the sign of $\delta\omega_{eg}$ can be reversed.

We begin our analysis with the Hamiltonian \hat{H} describing cold fermionic alkaline-earth atoms illuminated by a linearly polarized laser beam with bare Rabi frequency Ω_0 and trapped in an external potential $V(\mathbf{r})$ that is the same for g and e (i.e. at the ‘‘magic wavelength’’ [1]). Assuming that the atoms are polarized in a state with nuclear spin projection m_0 , we omit the nuclear spin label and, setting $\hbar = 1$, obtain [14, 15]

$$\hat{H} = \sum_{\alpha} \int d^3\mathbf{r} \hat{\Psi}_{\alpha}^{\dagger} \left(-\frac{1}{2M} \nabla^2 + V(\mathbf{r}) \right) \hat{\Psi}_{\alpha} + u_{eg}^{-} \int d^3\mathbf{r} \hat{\rho}_e \hat{\rho}_g + \omega_0 \int d^3\mathbf{r} (\hat{\rho}_e - \hat{\rho}_g) - \frac{\Omega_0}{2} \int d^3\mathbf{r} (\hat{\Psi}_e^{\dagger} e^{-i(\omega_L t - \mathbf{k} \cdot \mathbf{r})} \hat{\Psi}_g + \text{h.c.}). \quad (1)$$

Here $\hat{\Psi}_{\alpha}(\mathbf{r})$ is a fermionic field operator at position \mathbf{r} for atoms in electronic state $\alpha = g$ (1S_0) or e (3P_0), while $\hat{\rho}_{\alpha}(\mathbf{r}) = \hat{\Psi}_{\alpha}^{\dagger}(\mathbf{r})\hat{\Psi}_{\alpha}(\mathbf{r})$ is the corresponding density operator. Since polarized fermions are in a symmetric nuclear state, their s -wave interactions are characterized by only one scattering length a_{eg}^- , with the corresponding interaction parameter $u_{eg}^- = 4\pi\hbar^2 a_{eg}^-/M$, describing collisions between two atoms in the antisymmetric electronic state $|-\rangle = (|ge\rangle - |eg\rangle)/\sqrt{2}$. The laser with frequency ω_L and wavevector \mathbf{k} is detuned from the atom transition frequency ω_0 by $\delta = \omega_L - \omega_0$.

As in the experiment of Ref. [3], we assume that most atoms are frozen along one (longitudinal) z -direction, leaving in the remaining transverse x - y plane an isotropic 2D harmonic oscillator with frequency $\omega_x = \omega_y$. We can then write $\hat{\Psi}_{\alpha}(\mathbf{r}) = \phi_0^z(z) \sum_{\nu} \hat{c}_{\alpha\nu} \phi_{\nu_x}(x) \phi_{\nu_y}(y)$, where ϕ_{ν}^z and ϕ_{ν}

are, respectively, the longitudinal and the transverse harmonic oscillator eigenmodes and $\hat{c}_{\alpha\nu}^\dagger$ creates a fermion in mode $\nu = (\nu_x, \nu_y)$ and electronic level α . Following Refs. [3, 18], we assume that the probe is slightly misaligned from the z -direction: $\mathbf{k} = k_z \hat{z} + k_x \hat{x}$ with $|k_x/k_z| \ll 1$. Defining then $\Omega_{\nu,\nu'} = \Omega_0 e^{-\eta_z^2/2} L_0(\eta_z^2) \langle \phi_\nu(x) | e^{ik_x x} | \phi_{\nu'}(x) \rangle$, where $\eta_i = k_i \sqrt{\frac{\hbar}{2m\omega_i}} \ll 1$ are the Lamb-Dicke parameters and L_n are Laguerre polynomials [21], laser induced sideband transitions can be neglected if $\Omega_{\nu,\nu' \neq \nu} \ll \omega_x$. In this regime, \hat{H} can be rewritten in the rotating frame as

$$\begin{aligned} \hat{H} = & -\delta \sum_{\nu} \hat{n}_{e\nu} + \sum_{\nu,\alpha} E_{\nu} \hat{n}_{\alpha\nu} - \sum_{\nu} \frac{\Omega_{\nu x}}{2} (\hat{c}_{g\nu}^\dagger \hat{c}_{e\nu} + \text{h.c.}) \\ & + u_{eg}^- \sum_{\nu_1 \nu_2 \nu_3 \nu_4} A_{\nu_1 \nu_2 \nu_3 \nu_4} \hat{c}_{e\nu_1}^\dagger \hat{c}_{e\nu_2} \hat{c}_{g\nu_3}^\dagger \hat{c}_{g\nu_4}, \end{aligned} \quad (2)$$

where $A_{\nu_1 \nu_2 \nu_3 \nu_4} = \int (\phi_0^\dagger)^4 dz \int \prod_j \phi_{\nu_{jx}} dx \int \prod_j \phi_{\nu_{jy}} dy$, $\hat{n}_{\alpha\nu} = \hat{c}_{\alpha\nu}^\dagger \hat{c}_{\alpha\nu}$, $\Omega_{\nu x} = \Omega_0 L_{\nu_x}(\eta_x^2) L_0(\eta_z^2) e^{-(\eta_x^2 + \eta_z^2)/2}$, and E_{ν} are single-particle energies.

Many interaction terms in Eq. (2) can be ignored provided that the interaction is weaker than ω_x and that the 2D oscillator is slightly anharmonic as in the experiment of Ref. [3]. Furthermore, we note that unless $\nu_1 = \nu_2$ and $\nu_3 = \nu_4$, $|\int \phi_{\nu_1}^2 \phi_{\nu_3}^2| \gg |\int \prod_j \phi_{\nu_j}|$. As a result, the interaction is dominated by the terms where (ν_1, ν_3) is equal to (ν_2, ν_4) , $(\nu_{4x}, \nu_{2y}, \nu_{2x}, \nu_{4y})$, $(\nu_{2x}, \nu_{4y}, \nu_{4x}, \nu_{2y})$, or (ν_4, ν_2) , which describe the exchange of modes along neither direction, along x , along y , and along both directions, respectively. Postponing the study of the terms exchanging modes along one direction only, the remaining terms conserve the number of particles per mode ν . Assuming there is only one atom in each of N non-empty modes $\vec{\nu} = \{\nu_1, \dots, \nu_N\}$, as is the case if all atoms are initially in the same internal state, \hat{H} can then be reduced to a spin-1/2 model describing these modes:

$$\hat{H}_S = -\delta \hat{S}_z - \sum_{\nu} \Omega_{\nu x} \hat{S}_x^{\nu} - \sum_{\nu \neq \nu'} U_{\nu\nu'} (\vec{S}^{\nu} \cdot \vec{S}^{\nu'} - 1/4). \quad (3)$$

Here $U_{\nu\nu'} = u_{eg}^- A_{\nu\nu\nu\nu'}$, $\vec{S}^{\nu} = \frac{1}{2} \sum_{\alpha,\alpha'} \hat{c}_{\alpha\nu}^\dagger \vec{\sigma}_{\alpha\alpha'} \hat{c}_{\alpha\nu}$, where $\vec{\sigma}$ are Pauli matrices in the $\{e, g\}$ basis, $\hat{S}_{i=x,y,z} = \sum_{\nu} \hat{S}_i^{\nu}$, and constant terms were dropped. \hat{H}_S is reminiscent of solid-state spin Hamiltonians, which can also feature long-range interactions and rich nonequilibrium dynamics [22].

The rotational invariance of the interaction term in \hat{H}_S ($\propto U_{\nu\nu'}$) is key to understanding some of the basic features of the model. The interaction term is diagonal in the collective angular momentum basis $|S, M, q\rangle$, satisfying $\hat{S}^2 |S, M, q\rangle = S(S+1) |S, M, q\rangle$ and $\hat{S}_z |S, M, q\rangle = M |S, M, q\rangle$, with $S = 0, \dots, N/2$ and $-S \leq M \leq S$. Here the extra label q is required to uniquely specify each state. The fully symmetric (Dicke) $S = N/2$ states do not interact. They are unique and the label q can be omitted for them.

For a homogeneous excitation, $\Omega_{\nu} = \bar{\Omega}$, the term $\sum_{\nu} \Omega_{\nu x} \hat{S}_x^{\nu}$ commutes with \hat{S}^2 , the interaction energy is con-

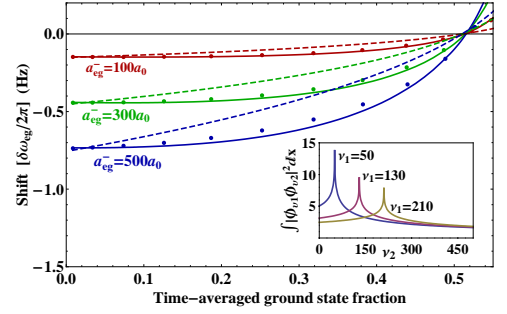


FIG. 1: (color online) CFS, $\delta\omega_{eg}/(2\pi)$, at resonant transfer, for different a_{eg} (in Bohr radii, a_0). The time-averaged ground state fraction was varied by changing t_f . The solid lines were calculated by thermally averaging N_g computed from Eq. (3), and the dots by a single realization of $\vec{\nu}$ randomly chosen out of those satisfying $\Delta\Omega(\vec{\nu}) = \langle \Delta\Omega \rangle_T$, $\bar{\Omega}(\vec{\nu}) = \langle \bar{\Omega} \rangle_T$, and $\bar{U}(\vec{\nu}) = \langle U \rangle_T$. The dashed lines show Eq. (5) evaluated at thermally averaged parameters. Here $N = 7$, $T = 1\mu\text{K}$, $\langle \Delta\Omega \rangle_T / \langle \bar{\Omega} \rangle_T = 0.2$ and $\bar{\Omega} = 6\pi/(80\text{ ms})$. The inset shows $\int \phi_{\nu_1}^2(x) \phi_{\nu_2}^2(x) dx$ in arbitrary units.

served, and no CFS will be observed provided the initial state is an eigenstate of the interaction or a classical mixture of them, consistent with Ref. [17]. If the system is prepared in the Dicke manifold, states with $S < N/2$ are never populated and the ground state population evolves collectively as $N_g^{(0)}(t, \delta) = N \frac{\bar{\Omega}^2}{\bar{\Omega}^2 + \delta^2} \sin^2\left(\frac{t\sqrt{\bar{\Omega}^2 + \delta^2}}{2}\right)$, where the superscript (0) indicates a homogeneous excitation.

In the presence of excitation inhomogeneity, there are two simple limiting cases where CFSs are absent: the non-interacting regime and the strongly interacting regime where interactions dominate over Rabi frequency inhomogeneity. The suppression of CFSs in the latter case is a consequence of the large energy gap between states with different S , which brings S -changing transitions out of resonance [23]. In the intermediate interaction regime, on the contrary, the excitation inhomogeneity cannot be ignored. It will transfer atoms between states with different S generating a net CFS even at zero temperature.

In most experiments, e.g. Ref. [3], $\delta\omega_{eg}$ is measured by first locking the spectroscopy laser at two points, $\delta_{1,2}$, of equal height in the transition lineshape (equal final ground state fraction under the initial condition of all atoms in state e) and then determining the change in the mean frequency as the interaction parameters or density are varied, $\delta\omega_{eg} = (\delta_1 + \delta_2)/2$. Note that for a homogeneous excitation $N_g^{(0)}(t, \delta) = N_g^{(0)}(t, -\delta)$ and therefore $\delta\omega_{eg} = 0$. Defining $\bar{\Omega}(\vec{\nu})$ to be the mean Rabi frequency over modes $\vec{\nu}$ and treating $\sum_{\nu} (\Omega_{\nu x} - \bar{\Omega}(\vec{\nu})) \hat{S}_x^{\nu}$ as a perturbation, we write $N_g(t_f, \delta)$ as $N_g^{(0)}(t_f, \delta) + N_g^{(2)}(t_f, \delta)$ (the first order term vanishes), Taylor expand it around $\pm\delta_1^{(0)}$, and obtain

$$\delta\omega_{eg} \approx \frac{N_g^{(2)}(t_f, -\delta_1^{(0)}) - N_g^{(2)}(t_f, \delta_1^{(0)})}{2 \frac{\partial N_g^{(0)}(t_f, \delta)}{\partial \delta} \Big|_{\delta_1^{(0)}}}. \quad (4)$$

To proceed further, we note that $U_{\nu\nu'}$ is a slowly varying function of $|\nu_i - \nu'_i|$ ($i = x, y$) [see Fig. 1 (inset)], except within a narrow range near $\nu_i = \nu'_i$. Provided $k_B T \gtrsim N\omega_z$ (which was satisfied in Ref. [3]), the occupied modes $\vec{\nu}$ are sufficiently sparse for the behavior of $U_{\nu_i\nu_j}$ to be dominated by its slowly varying part. Therefore, we can approximate $U_{\nu_i\nu_j} \rightarrow \bar{U}(\vec{\nu})$. Under this approximation, the states with $S = N/2 - 1$, so called spin-wave states, are separated in energy from the Dicke states by $\bar{U}(\vec{\nu})N$ and are the only states excited to first order by the vector perturbation operator $\sum_{\nu} (\Omega_{\nu_x} - \bar{\Omega}(\vec{\nu})) \hat{S}_x^{\nu}$. This allows us to obtain an analytic expression for $\delta\omega_{eg}$ that depends on $\Omega_{\nu_{ix}}$ only through $\bar{\Omega}(\vec{\nu})$ and $\Delta\Omega(\vec{\nu})$, the root-mean-square Rabi frequency. This expression is particularly simple and illuminating when evaluated at resonant population transfer ($\delta_1^{(0)} \rightarrow 0$):

$$\delta\omega_{eg} \Big|_{\delta_1^{(0)} \rightarrow 0} = -\frac{\Delta\Omega^2 N\bar{U}}{\bar{\Omega}^2} \frac{\sin(\mathcal{A})}{\mathcal{A}} \frac{\sin[(N\bar{U})t_f]}{(N\bar{U})t_f} f(\bar{\Omega}, t_f, N\bar{U}). \quad (5)$$

Here $\mathcal{A}(\vec{\nu}) = \bar{\Omega}(\vec{\nu})t_f$ is the pulse area and $f(\bar{\Omega}, t_f, N\bar{U}) = \frac{1 - \bar{\Omega}/(N\bar{U}) \tan(t_f(N\bar{U})/2) \cot(\mathcal{A}/2)}{(1 - (N\bar{U})^2/\bar{\Omega}^2)[4 \sin^2(\mathcal{A}/2)/\mathcal{A}^2 - \sin(\mathcal{A})/\mathcal{A}]}$. The dependence of \bar{U} , $\bar{\Omega}$, and $\Delta\Omega$ on $\vec{\nu}$ is implied. We now make a few important remarks: (a) In the limit $t_f \rightarrow 0$ ($N_e \rightarrow 1$), Eq. (5) reproduces the mean-field expression $\delta\omega_{eg} \rightarrow -\frac{(\Delta\Omega)^2 N\bar{U}}{\bar{\Omega}^2} \propto -N\bar{U}G_{ge}^{(2)}[t_f \rightarrow 0, \delta \rightarrow 0]$ [3, 18]. (b) $\delta\omega_{eg}$ depends on the time-averaged population difference, $\langle N_g - N_e \rangle_{t_f} = \frac{1}{t_f} \int_0^{t_f} (N_g(\tau) - N_e(\tau)) d\tau|_{\delta=0, \Delta\Omega=0} = -\frac{N \sin(\mathcal{A})}{\mathcal{A}}$ and exactly vanishes at $\mathcal{A} = \pi$ when $\langle N_g \rangle_{t_f} = \langle N_e \rangle_{t_f}$. (c) For a fixed pulse area \mathcal{A} , as $t_f \rightarrow 0$, the frequency shift vanishes as $\delta\omega_{eg} \rightarrow -(\Delta\Omega t_f)^2 N\bar{U} \cot[\mathcal{A}/2]/(2\mathcal{A})$, implying that in order to experience a CFS atoms need time to feel the excitation inhomogeneity. (d) At finite times $t_f N\bar{U} \gtrsim 1$ and $N\bar{U} \gg \bar{\Omega}$, $\delta\omega_{eg} \propto \frac{\sin[t_f(N\bar{U})]}{(N\bar{U})^2}$ reproducing the expected suppression in the strongly interacting limit.

So far we have assumed a fixed set of populated modes, $\vec{\nu}$. At finite temperature, expectation values need to be calculated by averaging over all possible combinations of modes $\{\vec{\nu}\}$ weighted according to their Boltzmann factor. However, since the quantities $\Delta\Omega(\vec{\nu})$, $\bar{\Omega}(\vec{\nu})$, and $\bar{U}(\vec{\nu})$ are sharply peaked around their thermal averages, to a good approximation, $\langle N_g \rangle_T$ and thus $\langle \delta\omega_{eg} \rangle_T$ can be calculated by replacing $\Delta\Omega(\vec{\nu}) \rightarrow \langle \Delta\Omega \rangle_T$, $\bar{\Omega}(\vec{\nu}) \rightarrow \langle \bar{\Omega} \rangle_T$, and $\bar{U}(\vec{\nu}) \rightarrow \langle \bar{U} \rangle_T$. Here $\langle O \rangle_T = \frac{\sum_{\vec{\nu}} O(\vec{\nu}) e^{-E(\vec{\nu})/(k_B T)}}{\sum_{\vec{\nu}} e^{-E(\vec{\nu})/(k_B T)}}$. The validity of this approximation is demonstrated in Fig. 1, which also shows that Eq. (5) is in fair agreement with Eq. (3).

Experimentally it is hard to measure CFSs close to resonant population transfer due to the small signal-to-noise ratio, and instead the probe laser is generally locked at a finite detuning [3]. Away from $\delta_1^{(0)} = 0$, we have to consider the more general expression given by Eq. (4), and an intuitive interpretation is not straightforward. The interaction induced asymmetry in the lineshape not only can change the sign of the frequency shift, but, in general, makes CFS a very sensitive function of $\langle \mathcal{A} \rangle_T$, $\delta_1^{(0)}$, and $\langle N\bar{U} \rangle_T$. In particular, the solid lines in Fig. 2

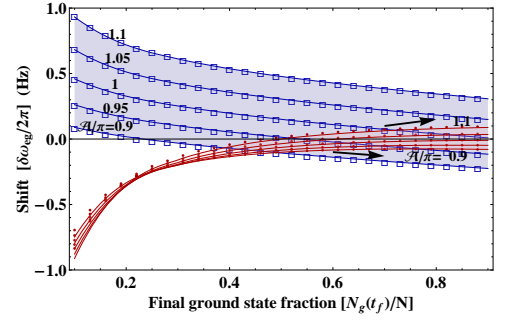


FIG. 2: (color online) CFS for different pulse areas, \mathcal{A} . The final ground state fraction, $N_g(t_f)/N$, was varied by changing the detuning. Here four spatial modes at the corners of a square in the ν_x - ν_y plane, $\nu_1 = (30, 43)$, $\nu_2 = (101, 71)$, $\nu_3 = (30, 71)$, and $\nu_4 = (101, 43)$, were assumed with $N = 2$ atoms occupying ν_1 and ν_2 at $t = 0$. The solid blue (red) lines, for $\bar{U}N/\bar{\Omega} = 1$ (3.25) and $t_f = \pi/\Omega_0 = 7$ ms, were obtained using Eq. (2), which allows to populate ν_3 and ν_4 . The empty squares (dots) were obtained using \hat{H}_S with an effective $\Omega_0^{eff} = \Omega_0/2$ and $t_f^{eff} = \pi/\Omega_0^{eff}$.

show the CFS as a function of the ground state fraction at t_f , computed using Eq. (2) for two atoms and four spatial modes. For weak repulsive interactions $0 < \langle N\bar{U} \rangle_T \lesssim \langle \bar{\Omega} \rangle_T$ (blue lines) and pulse areas greater than π , $\delta\omega_{eg} > 0$ for any detuning and approaches zero only as $\delta_1^{(0)} \rightarrow 0$ and $\mathcal{A} \rightarrow \pi$ (consistently with remark b above). For $\mathcal{A} < \pi$, $\delta\omega_{eg}$ changes sign as a function of $N_g(t_f)$, and the zero crossing point moves towards smaller $N_g(t_f)$ with decreasing pulse area. For stronger interactions $\langle N\bar{U} \rangle_T > \langle \bar{\Omega} \rangle_T > 0$ (red lines), while at large $N_g(t_f)$ the sign of $\delta\omega_{eg}$ also depends on whether $\langle \mathcal{A} \rangle_T$ is larger or smaller than π , at small $N_g(t_f)$ the magnitude of the CFS becomes less sensitive to pulse area variations and recovers the expected negative sign for repulsive interactions (since at $t = 0$ all atoms are in e). All these conclusions are consistent with the measurements reported in Ref. [3] since $\sim 10\%$ variations in \mathcal{A} over the course of a day could not be excluded.

We now discuss the effect of the terms whose omission in the derivation of Eq. (3) was not justified: the terms exchanging modes along one direction only. As shown in Fig. 2 for the case of two atoms occupying four modes, the spin model \hat{H}_S (dots) reproduces the result of Eq. (2) (lines) very well provided that we reduce Ω_0 in \hat{H}_S by a factor of 2: $\Omega_0^{eff} = \Omega_0/2$. This approximate result can be derived analytically by noting that the ν_1 - ν_2 singlet ($|-\rangle$) from the spin model is replaced in Eq. (2) by the symmetric linear combination of the ν_1 - ν_2 and the ν_3 - ν_4 singlets. We have checked that for $N = 3$ and 4 with N^2 modes, \hat{H}_S with $\Omega_0^{eff} = \alpha\Omega_0$ ($1/2 < \alpha < 1$) also reproduces well the results of Eq. (2).

Conjecturing the validity of \hat{H}_S with Ω_0^{eff} at larger N as well, we used \hat{H}_S to calculate the CFS for the parameters of Ref. [3]. The results are shown in Fig. 3. Our model gives reasonable agreement within the experimental data error bars for a range of scattering lengths $a_{eg}^- = (100 - 500)a_0$ with

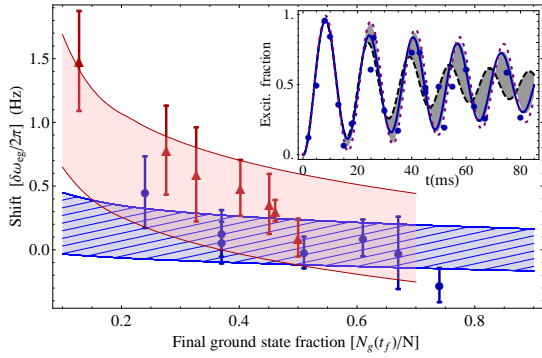


FIG. 3: (color online) CFS predicted by our spin model for $T = 1(3)\mu\text{K}$ and $\langle\Delta\Omega\rangle_T/\langle\bar{\Omega}\rangle_T = 0.15$ (0.42), determined from the Rabi flopping curves [see inset]. The blue (pink) shaded area shows the uncertainty in CFS for $T = 1(3)\mu\text{K}$, assuming a variation in pulse area of $\langle A \rangle_T/\pi = 1 \pm 0.1$. We used $\Omega_0^{eff} = 4\pi/80\text{ms}$, $t_f = \pi/\Omega_0^{eff}$, $N = 15$ [i.e. $\rho \sim 10^{11}\text{cm}^{-3}$], and $a_{eg}^- = 200a_0$. The circles (triangles) show the $T = 1(3)\mu\text{K}$ experimental data of Ref. [3] at $t_f = 80\text{ms}$ and $\rho \sim 10^{11}\text{cm}^{-3}$. Inset: The shaded area shows Rabi flopping curves calculated at $\langle\Delta\Omega\rangle_T/\langle\bar{\Omega}\rangle_T = 0.15$ for $a_{eg}^- = 0 - 600a_0$. The dashed black and solid blue lines correspond to two specific scattering lengths, $a_{eg}^- = 0$ and $200a_0$, respectively. The dotted purple line is for $\langle\Delta\Omega\rangle_T/\langle\bar{\Omega}\rangle_T = 0.05$ and $a_{eg}^- = 0$, while the blue circles are experimental data points from Ref. [3].

$\Omega_0^{eff} = 4\Omega_0$. The net effect of Ω_0^{eff} is to rescale the shift by a factor of four [28], which is justified by the exchanging-modes corrections discussed above and by the large (up to a factor of 5 [24]) uncertainty in the experimental determination of the density. We also note that in Ref. [3] $\langle\Delta\Omega\rangle_T$ was inferred by fitting Rabi oscillations with a non-interacting model. However, the inset of Fig. 3 shows that interactions modify Rabi oscillations and that the non-interacting model can underestimate $\langle\Delta\Omega\rangle_T$ by a factor as large as three. All these issues combined with the experimental uncertainty in pulse area complicate the determination of the magnitude of a_{eg}^- from the current data. Nevertheless, our model at least suggests it to be positive, $a_{eg}^- > 0$.

In addition to a_{eg}^- , there is another scattering length a_{eg}^+ , which characterizes collisions between a g and an e atom. a_{eg}^+ collisions require a symmetric electronic state and consequently an anti-symmetric nuclear spin configuration. Thus the interaction Hamiltonian describing g - e collisions beyond the polarized regime is [14, 15]

$$\hat{H}_{int} = u_{eg}^s \int d^3\mathbf{r} \hat{\rho}_e \hat{\rho}_g + u_{eg}^a \sum_{mm'} \int d^3\mathbf{r} \hat{\Psi}_{gm}^\dagger \hat{\Psi}_{em'}^\dagger \hat{\Psi}_{gm'} \hat{\Psi}_{em}. \quad (6)$$

Here $u_{eg}^{s,a} = (u_{eg}^+ \pm u_{eg}^-)/2$, s (a) stands for symmetric (anti-symmetric), $m, m' = -I, \dots, I$ label the nuclear Zeeman levels, $u_{eg}^+ = 4\pi\hbar^2 a_{eg}^+/M$, and $\hat{\rho}_\alpha(\mathbf{r}) = \sum_m \hat{\Psi}_{\alpha m}^\dagger(\mathbf{r}) \hat{\Psi}_{\alpha m}(\mathbf{r})$.

We now propose how to estimate a_{eg}^+ experimentally. The method is identical to that of Ref. [3] except that probe light polarization should be circular instead of linear. The idea is to Rabi interrogate an ensemble of $|e, m_0\rangle$ atoms with a cir-

cularly polarized probe driving the $|e, m_0\rangle - |g, m_0 + 1\rangle$ transition. If $a_{eg}^+ = a_{eg}^-$, then $u_{eg}^a = 0$ and the dynamics of the system are identical to the ones described above, except that one needs to identify $\{|e, m_0\rangle, |g, m_0 + 1\rangle\}$ as the spin basis. However, if $a_{eg}^+ \neq a_{eg}^-$, the term proportional to u_{eg}^a will populate $|e, m_0 + 1\rangle$ and $|g, m_0\rangle$. This issue can be overcome by applying an external magnetic field. If the applied magnetic field satisfies $B\mu_N\Delta g \gg \langle\bar{U}^a\rangle_T$, with μ_N the nuclear magneton, Δg the differential g -factor between e and g [25, 26], and $\langle\bar{U}^a\rangle_T$ the thermally averaged antisymmetric interaction, then the processes populating $|e, m_0 + 1\rangle$ and $|g, m_0\rangle$ will be energetically suppressed, and the dynamics will be identical to the ones in Ref. [3] with CFS proportional to u_{eg}^s . By comparing the CFS between the linearly and circularly polarized cases, one can in principle infer a_{eg}^+ .

In summary, fermionic clocks are sensitive to the CFS induced by excitation inhomogeneities. The CFS is sensitive to pulse area, detuning, and interaction strengths, but if measured close to resonant transfer, it is in qualitative agreement with the expected mean field expression. To improve the experimental resolution of the CFS, better control over pulse area variations is required. Rabi interrogation schemes can also be used to estimate a_{eg}^+ .

Note added in proof: While writing this paper, we learned about a related study of interaction frequency shifts in clock experiments [27].

We gratefully acknowledge conversations with and feedback from J. Ye, S. Blatt, G. Campbell, A. Ludlow, P. Julienne, and M. Lukin. This work was supported by NSF.

-
- [1] J. Ye, H. J. Kimble, and H. Katori, *Science* **320**, 1734 (2008).
 - [2] A. D. Ludlow et al., *Science* **319**, 1805 (2008).
 - [3] G. K. Campbell et al., *Science* **324**, 360 (2009).
 - [4] T. Akatsuka, M. Takamoto, and H. Katori, *Nature Phys.* **4**, 954 (2008).
 - [5] M. Takamoto and H. Katori, *J. Phys. Soc. Jpn.* **78**, 013301 (2009).
 - [6] T. Fukuhara, Y. Takasu, S. Sugawa, and Y. Takahashi, *J. Low Temp. Phys.* **148**, 441 (2007).
 - [7] T. Fukuhara, Y. Takasu, M. Kumakura, and Y. Takahashi, *Phys. Rev. Lett.* **98**, 030401 (2007).
 - [8] C. Lisdat et al., arXiv:0904.2515 (2009).
 - [9] Z. W. Barber et al., *Phys. Rev. Lett.* **100**, 103002 (2008).
 - [10] L. M. Lemke et al., arXiv:0906.1219 (2009).
 - [11] I. Reichenbach and I. H. Deutsch, *Phys. Rev. Lett.* **99**, 123001 (2007).
 - [12] D. Hayes, P. S. Julienne, and I. H. Deutsch, *Phys. Rev. Lett.* **98**, 070501 (2007).
 - [13] A. J. Daley, M. M. Boyd, J. Ye, and P. Zoller, *Phys. Rev. Lett.* **101**, 170504 (2008).
 - [14] A. V. Gorshkov et al., *Phys. Rev. Lett.* **102**, 110503 (2009).
 - [15] A. V. Gorshkov et al., arXiv:0905.2610v1 (2009).
 - [16] S. Gupta et al., *Science* **300**, 1723 (2003).
 - [17] M. W. Zwierlein, Z. Hadzibabic, S. Gupta, and W. Ketterle, *Phys. Rev. Lett.* **91**, 250404 (2003).
 - [18] S. Blatt et al., arXiv:0906.1419 (2009).

- [19] M. O. Oktel and L. S. Levitov, Phys. Rev. Lett. **83**, 6 (1999).
- [20] M. O. Oktel, T. C. Killian, D. Kleppner, and L. S. Levitov, Phys. Rev. A **65**, 033617 (2002).
- [21] D. J. Wineland and W. M. Itano, Phys. Rev. A **20**, 1521 (1979).
- [22] M. V. G. Dutt et al., Science **316**, 1312 (2007).
- [23] A. M. Rey, L. Jiang, M. Fleischhauer, E. Demler, and M. D. Lukin, Phys. Rev. A **77**, 052305 (2008).
- [24] S. Blatt, Private Communication (2009).
- [25] M. M. Boyd et al., Science **314**, 1430 (2006).
- [26] M. M. Boyd et al., Phys. Rev. A **76**, 022510 (2007).
- [27] K. Gibble, arxiv:0908.3147 (2009).
- [28] For fixed pulse areas, an effective bare Rabi frequency renormalizes the CFS according to the following scaling law

$$\delta\omega_{eg}(\Omega_0, \bar{U}, \delta) = \frac{\Omega_0}{\Omega_0^{eff}} \delta\omega_{eg}(\Omega_0^{eff}, \bar{U} \frac{\Omega_0^{eff}}{\Omega_0}, \delta \frac{\Omega_0^{eff}}{\Omega_0}).$$